Characterizing WR-8 Waveguide-to-CPW Probes Using Two Methods Implemented within the NIST Uncertainty Framework

Jeffrey A. Jargon[1], Uwe Arz[2], and Dylan F. Williams[1]

[1]National Institute of Standards and Technology, Boulder, CO 80305 USA
Tel.: +1.303.497.4961, Email: jargon@boulder.nist.gov
[2]Physikalisch-Technische Bundesanstalt, 38116 Braunschweig, Germany

***Abstract* — We individually characterize and provide uncertainties for a pair of WR-8 rectangular waveguide-to-coplanar waveguide (CPW) probes over a frequency range of 90 to 140 GHz utilizing two methods implemented within the NIST Microwave Uncertainty Framework. The first method consists of a two-tier approach, where a vector network analyzer (VNA) calibration is first performed in rectangular waveguide, and then a second-tier calibration is performed on-wafer. The second method determines the scattering parameters of the probes from two one-tier calibrations. We show that the two methods yield nearly equivalent results and uncertainties.**

***Index Terms* — Characterize, compare, coplanar waveguide, network analyzer, probe, rectangular waveguide, uncertainty.**

I. Introduction

Microwave probes are commonly used for high-frequency measurements of on-wafer devices. Characterizing these probes poses a challenge, because the two ports consist of different interconnecting environments – one is typically coaxial or rectangular waveguide, and the other is coplanar waveguide. Being noninsertable devices, probes cannot be characterized by use of a single vector network analyzer (VNA) calibration. This problem is similar to that of coaxial adapters containing two connectors of different sizes and/or the same sex. Several techniques have been developed over the years for characterizing noninsertable adapters, including the one-port Bauer-Penfield method [1], the adapter removal technique [2], and a host of other variants [3, 4]. These techniques have been modified for characterizing standard coplanar probes [5], as well as high-impedance probes [6].

In this paper, we compare two methods for characterizing WR-8 waveguide-to-coplanar waveguide (CPW) probes with uncertainties over a frequency range of 90 to 140 GHz. The first method employs a Bauer-Penfield-type two-tier approach [1, 6], where a VNA calibration is first performed in rectangular waveguide, and then a second-tier calibration is performed on-wafer. The second method is a technique that determines the scattering parameters of the probes from two one-tier calibrations. Both methods require post-processing of the data after the calibrations are performed.

Throughout the process of characterizing the probes, we utilize the NIST Microwave Uncertainty Framework [7, 8] to propagate uncertainties. This approach is based on a covariance-matrix uncertainty description that enables us to capture all of the S-parameter measurement uncertainties and statistical correlations between them [9]. By identifying and modeling the physical error mechanisms in the calibration standards, we can determine the statistical correlations between uncertainties at different frequencies. These covariance-based uncertainties can then be propagated into the uncertainties of the scattering parameters of the probes. This is particularly valuable when transforming from the frequency-domain to the time-domain.

In the following sections, we describe two methods for individually characterizing a pair of microwave probes, explain the measurement methodology and error mechanisms, and present our results.

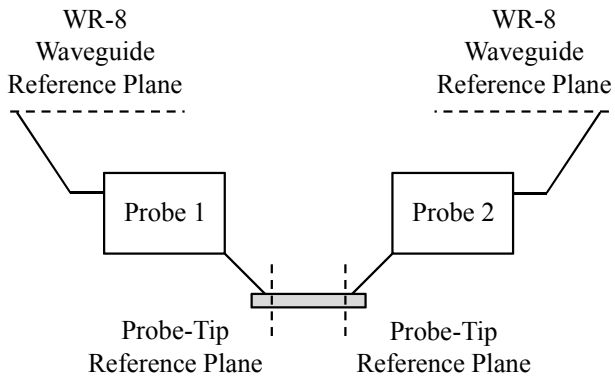

Fig. 1. Two WR-8 waveguide-to-CPW probes making contact to an on-wafer device.

II. Probe Characterization Procedures

A. Method 1: Two-Tier Approach

The first method employs a Bauer-Penfield-type two-tier approach [1, 6], where first a one-tier calibration is performed at a reference plane outside of the fixture. In our case, this is done at the WR-8 rectangular waveguide reference plane, shown in Figure 1. Next, two waveguide-to-CPW probes are connected between the waveguide planes, also shown in Figure 1. These probes are then contacted to on-wafer CPW calibration standards, and a second-tier calibration is performed at the probe-tip reference plane. By second-tier, we mean that the first-tier calibration performed at the WR-8 rectangular waveguide reference plane is used to correct the

measurements made of the on-wafer standards. This second-tier calibration maps measurements at the initial waveguide calibration reference plane to the final probe-tip reference plane on the wafer by means of two electrical two-port scattering parameters, which are often referred to as "error boxes." In this instance, the two error boxes describe the electrical characteristics of the two probes.

B. Method 2: One-Tier Approach

The second method is a technique that determines the scattering parameters of the probes from two one-tier calibrations. Similar to Method 1, a one-tier calibration is first performed at a reference plane outside of the fixture. Once again, this is done at the WR-8 rectangular waveguide reference plane, resulting in the determination of error boxes $\mathbf{S}_{W1}$ and $\mathbf{S}_{W2}$, illustrated in Figure 2. Here, '**S**' refers to the scattering matrix, the subscript 'W' refers to waveguide, and subscripts 1 and 2 refer to the left- and right-side ports, respectively. Next, two waveguide-to-CPW probes are connected between the waveguide planes, and the probes are then contacted to on-wafer CPW calibration standards. Here, a second one-tier calibration is performed at the probe-tip reference plane, resulting in the determination of error boxes $\mathbf{S}_{O1}$ and $\mathbf{S}_{O2}$, also illustrated in Figure 2. Here, the subscript 'O' refers to 'on-wafer.'

The scattering parameters of the probe on port 1 are calculated by multiplying the inverse of the port 1 error box of the waveguide calibration by the port 1 error box of the on-wafer calibration. This is achieved by first converting the S-parameters to transmission parameters, or T-parameters, so the matrices can be directly multiplied. Thus, in T-parameter form, $\mathbf{T}_{P1}= \mathbf{T}_{W1}^{-1}* \mathbf{T}_{O1}$, where the subscript 'P' refers to the probe. Finally, the S-parameters of the probe are determined by converting the T-parameters back to S-parameters, giving $\mathbf{S}_{P1}$. Likewise, the scattering parameters of the probe on port 2 are calculated by multiplying the port 2 error box of the on-wafer calibration by the inverse of the port 2 error box of the waveguide calibration. In T-parameter form, $\mathbf{T}_{P2}= \mathbf{T}_{O2}*\mathbf{T}_{W2}^{-1}$**.** After converting back to S-parameters, we have $\mathbf{S}_{P2}$.

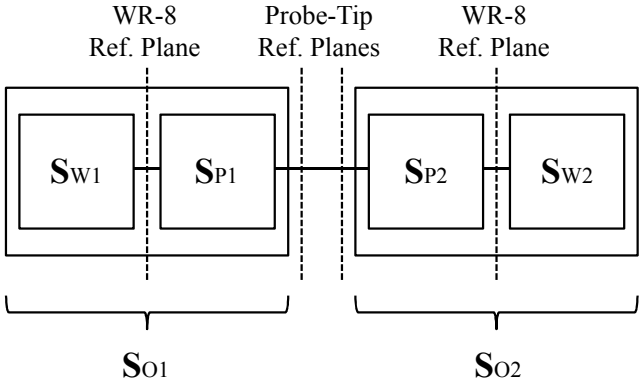

Fig 2. Error boxes in the one-tier approach.

III. Methodology

In order to compare the two methods for characterizing probes, we began by measuring the WR-8 standards. Our WR-8 calibration kit consisted of a sliding load, a flush short, a thru connection, and a delay line. In order to capture the repeatability of our connections, we measured the sliding load in both the upright and upside-down configurations, and the delay line was measured upright and upside-down in both the forward and backward directions. Using these measurements, along with their respective definitions (i.e., lengths, widths, etc.) and associated uncertainties, listed in Table I, we calibrated the VNA utilizing the NIST Microwave Uncertainty Framework, which resulted in a set of calibration coefficients along with uncertainties.

Table I. Physical error mechanisms of the WR-8 standards.

Mechanism (units)	Value ± Uncertainty (Distribution)
Thru Length (mm)	0 ± 0.005 (Rectangular)
Line Length (mm)	0.889 ± 0.005 (Rectangular)
Width (mm)	2.032 ± 0.005 (Rectangular)
Height (mm)	1.016 ± 0.005 (Rectangular)
Metal Resistivity Relative to Cu (unitless)	2 ± 1 (Rectangular)

Table II. Lengths and uncertainties of the on-wafer standards.

Line Designation	Length (μm) ± Uncertainty (Probability Distribution)
Thru	470 ± 1 (Rectangular)
Line 1	570 ± 1 (Rectangular)
Line 2	770 ± 1 (Rectangular)
Line 3	970 ± 1 (Rectangular)
Line 4	2470 ± 1 (Rectangular)
Line 5	7470 ± 1 (Rectangular)
Line 6	5470 ± 1 (Rectangular)
Line7	11470 ± 1 (Rectangular)
Offset Shorts	235 ± 1 (Rectangular)

Table III. Error mechanisms of the on-wafer standards.

Mechanism (units)	Value ± Uncertainty (Distribution)
Center-Conductor Width (μm)	15 ± 1 (Rectangular)
Gap Width (μm)	20 ± 1 (Rectangular)
Metal Thickness (μm)	0.36 ± 0.05 (Rectangular)
Ground-Plane Width (μm)	82 ± 1 (Rectangular)
Substrate Thickness (μm)	350 ± 10 (Rectangular)
Relative Dielectric Const.	46 ± 1 (Rectangular)
Metal Conductivity (S/m)	$2\times10^{7} \pm 1\times10^{7}$ (Rect.)
Substrate Loss Tangent	$1\times10^{-3} \pm 0.5\times10^{-3}$ (Rect.)

The NIST Microwave Uncertainty Framework [7, 8] is employed to construct models for the calibration standards, and is used for automatically propagating the uncertainties to the calibrated DUTs in conjunction with the calibration

engine, StatistiCAL™ [10, 11], which accommodates almost all coaxial, waveguide, and on-wafer standards, and enables a "mix and match" philosophy to VNA calibrations. For our WR-8 calibration, we assumed the thru, flush short and sliding load to be ideal, while the line was modeled using closed-form expressions for waveguides with finite metal conductivity [12].

Next, two GSG, waveguide-to-CPW probes were connected between the waveguide planes. The probes were then contacted to a $LiTaO_3$ wafer containing the on-wafer CPW calibration standards, consisting of a thru, an offset short, and seven lines of varying lengths. We use an electro-optic $LiTaO_3$ wafer, since it will be used with the probe under consideration in the NIST primary electro-optic sampling (EOS) system [13]. Table II lists the line lengths and associated uncertainties for the on-wafer standards, and Table III lists the other physical error mechanisms for the on-wafer standards. The on-wafer standards were modeled as lossy coplanar transmission lines that include dispersion and radiation [14]. It should be pointed out that some of the uncertainties are rough estimates based rather on experience and/or literature than experiments.

Both probe characterization procedures made use of the same measured data, thus eliminating any differences due to repeatability. In the two-tier approach, the first-tier calibration performed at the WR-8 rectangular waveguide reference plane was used to correct all of the measurements made on the on-wafer standards. And in the one-tier approach, both the WR-8 and on-wafer calibrations were performed as first-tier calibrations. Finally, we made use of a post-processor that is part of the NIST Microwave Uncertainty Framework to calculate the S-parameters and propagate uncertainties for both probe characterization methods.

IV. Results

If we model a microwave probe as a two-port circuit, its behavior is ideally described by a delay line in the frequency range specified by the manufacturer. This means that the values of the reflection coefficients (S_{11} and S_{22}) at both the waveguide input and the probe tip are very small, and the values of the transmission coefficients (S_{21} and S_{12}) are close to 1, or 0 dB. Figures 3 and 4 show the measured S-parameters of Probe 1 and 2, as determined by both characterization procedures. The dashed lines represent the S-parameters determined by the two-tier method, and the solid lines represent the S-parameters determined by the one-tier method. The two approaches yield nearly identical results. The transmission coefficients show a few decibels of loss, which is expected at these high frequencies. Furthermore, the values of S_{22} are higher than those of S_{11} for Probe 1, which is also not surprising, considering the probe is usually better matched at the waveguide input than at the probe tip. Likewise, the values of S_{11} are higher than those of S_{22} for Probe 2, since the waveguide input and the probe tip are reversed.

To see how the two approaches compare in more detail, we plot the magnitudes and phases of some of the individual S-parameters. Figures 5-8 display the magnitudes and phases of S_{21} and S_{22} for Probe 1. All four graphs show that the two approaches agree well within their respective 95 % confidence intervals.

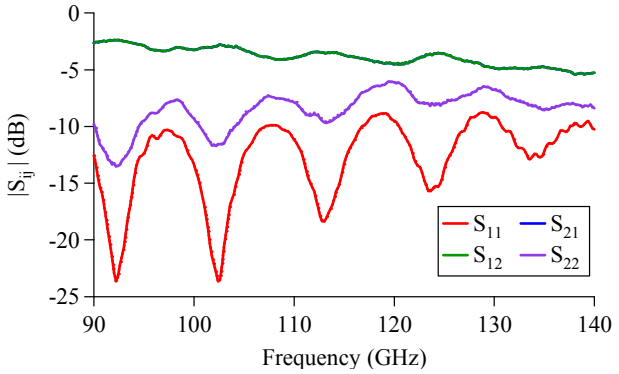

Fig. 3. Magnitudes of measured S-parameters for Probe 1 by use of both approaches. The dashed lines represent the two-tier method and the solid lines represent the one-tier method.

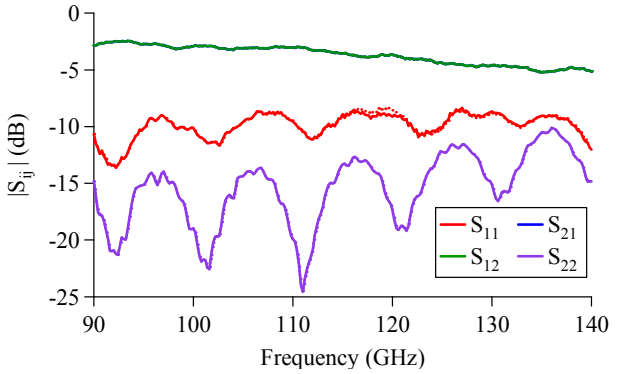

Fig. 4. Magnitudes of measured S-parameters for Probe 2 by use of both approaches.

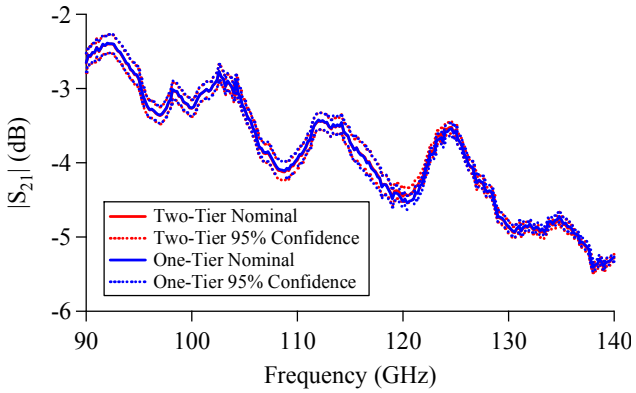

Fig. 5. Magnitude of S_{21} for Probe 1 by use of both approaches with 95 % confidence intervals.

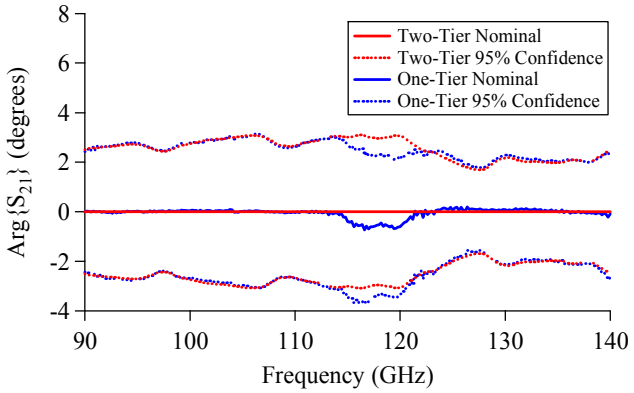

Fig 6. Phase of S_{21} for Probe 1 by use of both approaches with 95 % confidence intervals, normalized to the two-tier nominal measurements.

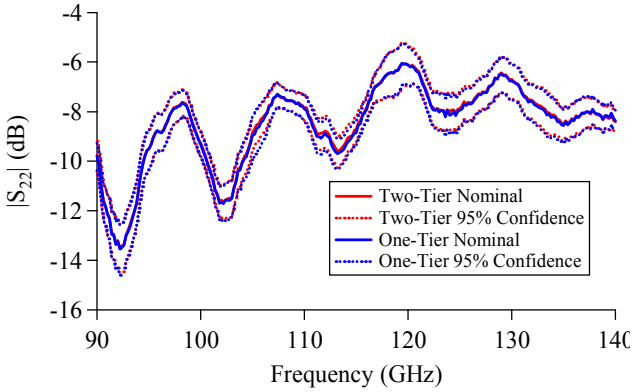

Fig. 7. Magnitude of S_{22} for Probe 1 by use of both approaches with 95 % confidence intervals.

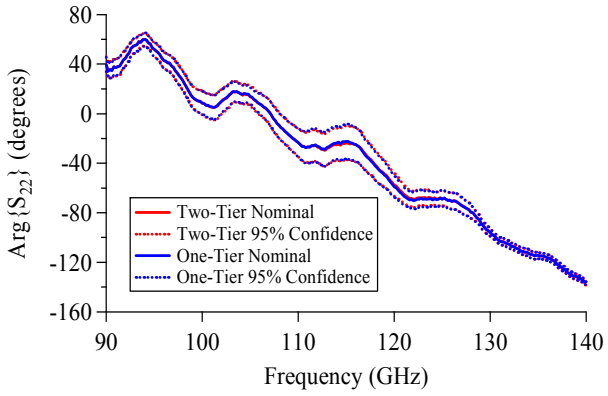

Fig. 8. Phase of S_{22} for Probe 1 by use of both approaches with 95 % confidence intervals.

V. Conclusion

We have individually characterized and provided uncertainties for a pair of WR-8 waveguide-to-CPW probes. Although there may be more effects to be considered in a final uncertainty budget, we believe our assumptions covered the major error contributions and were sufficient for comparing the methods. Furthermore, our results provide credence that both approaches for characterizing microwave probes yield nearly equivalent results and uncertainties. This is not surprising, since the two methods should yield identical results assuming there is no coupling between the VNA ports and the switch-terms are constant.

Acknowledgement

The authors thank Arkadiusz Lewandowski and Michael Janezic for their helpful comments regarding the preparation of this manuscript. This work was supported by the U.S. Department of Commerce, and is not subject to U.S. copyright.

References

[1] R. F. Bauer and P. Penfield, Jr., "De-Embedding and Unterminating," *IEEE Trans. Microwave Theory Tech.*, vol. MTT-22, no. 3, pp. 282-288, Mar. 1974.

[2] "Measuring Noninsertable Devices," Hewlett-Packard Company, Santa Rosa, CA, Product Note 8510-13, Aug. 1988.

[3] J. Randa, W. Wiatr, and R. L. Billinger, "Comparison of Adapter Characterization Methods," *IEEE Trans. Microwave Theory Tech.*, vol. 47, no. 12, pp. 2613-2620, Dec. 1999.

[4] J. Martens, "Common Adapter/Fixture Extraction Techniques: Sensitivities to Calibration Anomalies," 74th ARFTG Microwave Measurements Conference, Dec. 2009, Broomfield, CO.

[5] U. Arz and D. Schubert, "Coplanar Microwave Probe Characterization: Caveats and Pitfalls," 67th ARFTG Microwave Measurements Conference, pp. 214-218, June 2006, San Francisco, CA.

[6] U. Arz, H. C. Reader, P. Kabos, and D. F. Williams, "Wideband Frequency-Domain Characterization of High Impedance Probes," 58th ARFTG Microwave Measurements Conference, pp. 214-218, Nov. 2011, San Diego, CA.

[7] NIST Microwave Uncertainty Framework, Beta Version, D. F. Williams, http://www.nist.gov/pml/electromagnetics/related-software.cfm, 2012.

[8] J. A. Jargon, D. F. Williams, T. M. Wallis, D. X. LeGolvan, and P. D. Hale, "Establishing Traceability of an Electronic Calibration Unit Using the NIST Microwave Uncertainty Framework," 79th ARFTG Microwave Measurement Conference, pp. 32-36, Montreal, CANADA, Jun. 2012.

[9] A. Lewandowski, D. F. Williams, P. D. Hale, C. M. Wang, and A. Dienstfrey, "Covariance-Matrix-Based Vector-Network-Analyzer Uncertainty Analysis for Time-and Frequency-Domain Measurements," *IEEE Trans. Microwave Theory Tech*., vol. 58, no. 7, pp. 1877-1886, July 2010.

[10] StatistiCAL VNA Calibration Software Package, D. F. Williams, http://www.nist.gov/pml/electromagnetics/related-software.cfm, 2012.

[11] D.F. Williams, C.M. Wang, and U. Arz, "An Optimal Vector-Network-Analyzer Calibration Algorithm," *IEEE Trans. Microwave Theory and Tech*., vol. 51, no. 12, pp. 2391 2401, Dec. 2003.

[12] R. E. Collin, *Foundations for Microwave Engineering*, Second Edition, IEEE Press, 2001.

[13] P. D. Hale, D. F. Williams, A. Dienstfrey, C. M. Wang, J. A. Jargon, D. Humphreys, M. Harper, H. Füser, and M. Bieler, "Traceability of High-Speed Electrical Waveforms at NIST, NPL, and PTB," 2012 Conference on Precision Electromagnetic Measurements Digest, pp. 522-523, Washington, DC, Jul. 2012.

[14] F. Schnieder, T. Tischler, and W. Heinrich "Modeling Dispersion and Radiation Characteristics of Conductor-Backed CPW with Finite Ground Width" *IEEE Trans. Microwave Theory Tech*., vol. 51, no. 1, pp. 137-143, Jan. 2003.